Ontogenesis

Eco-evolutionary perspective on life history complexity

Hin, V.

Chapter 3

Evolution of Metabolic Scaling

Vincent Hin

André M. de Roos

Manuscript in preparation

Abstract

Theories about the metabolic organization of organisms use constraints on energy supply or reserve mobilization to predict how metabolic rate scales with body mass during ontogeny. Observed variation in the ontogenetic scaling of metabolism with body mass can be explained through changes in the organism's shape during ontogeny. Although observed variation in the scaling of metabolic rate with body mass is significant and depends on ecological and physiological characteristics, the adaptive consequences of such variation has received little attention. Here, we address this by using a size-structured consumer-resource model with a dynamic energy budget describing consumer energetics. We study adaptive dynamics of the body size scaling of two processes that contribute significantly to metabolic rate: energy supply (assimilation) and maintenance metabolism. Assimilation is described by a type-II functional response, which depends on two processes that each have a separate scaling relation with body size: the maximum ingestion rate and the attack rate. We either use a juvenile-adult trade-off, in which an increase of a metabolic process in one consumer life stage results in a decrease in the other consumer life stage, or an energetic trade-off, in which increasing assimilation is associated with increasing metabolic costs. We show that independent of the considered trade-off, the scaling exponents related to energy supply converge towards the same value over evolutionary time. Furthermore, under a juvenile-adult trade-off the scaling of assimilation and maintenance metabolism converge such that the food threshold for starvation becomes independent of body size. Under an energetic trade-off, however, the maintenance scaling is unaffected by the scaling of assimilation. We discuss how these results relate to the variation in the scaling of metabolic rate with body size.

3.1 – Introduction

Understanding the metabolic organization of organisms provides a powerful way to unravel the interplay between hierarchical levels of biological complexity (Brown et al. 2004; Marquet et al. 2004; Sousa et al. 2008, 2010). Many processes at the population, community and ecosystem level depend on how individual organisms take up, convert and use energy and nutrients from the environment, *i.e.* on their metabolism (Enquist et al. 2003; Kooijman 2010; Martin et al. 2013; Nisbet et al. 2008; Van der Meer 2006). Models on the metabolism of individuals that are useful for ecology take the approach of ignoring complex metabolic networks containing thousands of interacting metabolites and instead apply the principles of mass and energy conservation while considering a limited number of biomass pools (Jusup et al. 2016; Kooijman 2001, 2010). The two main approaches are the Dynamic Energy Budget theory (DEB; Kooijman 2010) and the Metabolic Theory of Ecology (MTE; Brown et al. 2004). In recent years the MTE has been successful in linking different levels of biological organization through the metabolism of individuals (Brown et al. 2004; Enquist et al. 2003; Sibly et al. 2012), but the idea of explaining higher-level patterns from individual-level energetics already dates back to the beginning of DEB theory (Kooijman and Metz 1984; Metz and Diekmann 1986).

The main determinant of an organism's metabolism is its body size and considerable research effort has been made to quantify the precise relationship of metabolic rate with body size as organisms grow (Glazier 2005, 2006). Such an ontogenetic scaling relation is often quantified with the power function $B = aM^b$, where B is metabolic rate, M is body mass across ontogeny, b is the scaling exponent and a is a proportionality constant that can depend on temperature (Gillooly et al. 2001; Zuo et al. 2012). Both DEB and MTE propose an explanation for the value of b and although the quantitative predictions of the two theories overlap, they do so for different reasons (Kearney and White 2012; Kooijman and Metz 1984; Maino et al. 2014; Van der Meer 2006).

The simplest DEB variant (the standard DEB model; Kooijman 2010) describes an isomorphically growing organism in terms of two individual state variables that represent different biomass pools: reserve and structure. Growth in structure is proportional to the difference between energy assimilation, which scales with the surface area of structure, and maintenance requirements, which is proportional to structural volume. Under constant food this leads to a Von Bertalanffy growth pattern in body length (Kooijman and Metz 1984). According to DEB theory, whole-organism metabolic rate equals the rate of all chemical transformations in an organism, which is usually quantified as heat production (Kooijman 2014; Sousa et al. 2008). Different processes contribute to this, such as overheads for feeding and digestion (specific-

dynamic action or heat-increment of feeding), overheads for growth, maintenance costs and (for endotherms) energy spent on thermogenesis (Kooijman 2014). The whole-organism metabolic rate is therefore a combination of processes that scale with body surface (assimilation and thermogenesis in endotherms) and those that scale with body volume (maintenance rate) (Kooijman 1986; Van der Meer 2006). Hence, standard DEB predicts a value of b in between two-thirds and one for growing organisms.

In the MTE, metabolic rate is defined as the rate at which organisms take up, transform and expend energy and materials (Brown et al. 2004) and is assumed to scale with an exponent of 0.75 to body mass (Savage et al. 2004; West et al. 2001). This three-quarters scaling relationship is derived from an optimization principle on the delivery of energy and materials from a central source through a space-filling, fractal-like distribution network (e.g. the cardiovascular system) towards the service regions where the metabolic work is done (Banavar et al. 1999, 2010; West 1997). The limitation of the distribution network is independent of species identity and $b = 0.75$ is therefore predicted to hold between fully grown individuals of different species (interspecific scaling, also referred to as Kleiber's law) and across ontogeny within species (ontogenetic scaling, but see Makarieva et al. 2009). During ontogenetic growth, the metabolic rate is assumed to control the rate of energy supply to cells and as such, constrains the amount of metabolic work that an organism can do (Brown et al. 2004; West et al. 2001). The energy supply is used for both maintenance of existing biomass and for the overhead costs of synthesizing new biomass in growing organisms (West et al. 2001). As in DEB theory, maintenance costs per unit biomass are assumed to be independent of body mass and maximum body size is reached when all metabolic power is spent on maintenance (Hou et al. 2011, 2008; West et al. 2001). While the metabolic rate fuels the maintenance costs and growth overheads, the generated biomass that is assembled into growing organisms and that is therefore not dissipated as heat, is derived from assimilated food (Hou et al. 2011, 2008; Makarieva et al. 2004). The rate of food assimilation does not follow a power law scaling relation, because it is assumed to match the metabolic rate plus the energy stored in newly assimilated biomass (Hou et al. 2011, 2008). The ontogenetic growth model of MTE therefore describes a demand-driven metabolic organization and is indeed mostly used to model ontogenetic growth of birds and mammals (Hou et al. 2011; West et al. 2004).

Substantial and consistent variation in b has been observed in many groups of animals, and this variation has been linked to several ecological, physiological and environmental factors (Bokma 2004; Caruso et al. 2010; Glazier 2005, 2009; Glazier et al. 2011, 2015; Killen et al. 2010, 2016; Ohlberger et al. 2012*b*). For example, scaling exponents of standard metabolic rate are significantly larger in pelagic invertebrate

species than in non-pelagic (Glazier 2005). Also, Ohlberger et al. (2012*b*) showed that evolutionary adaptive responses to temperature can affect the scaling of metabolic rate with body mass in fishes. While in the MTE the scaling is assumed fixed at $b = 0.75$, DEB allows for more variation in scaling exponents due to varying contributions of the different processes that lead to heat dissipation. It therefore seems that the observed variation in b can be better accommodated in DEB theory, than in the MTE. However, changes in b can be explained by MTE through changes in the shape of the organism during ontogenetic growth. Changes in shape alter the spatial dimensionality of the ontogenetic growth, which affects the predicted scaling of metabolic rate with body size (Kearney and White 2012). As West (1997); West et al. (1999) derive, $b = {}^{D}/_{(D+1)}$, where D denotes this spatial dimensionality. Hence, for isomorphically growing animals that exhibit equally rapid growth in 3 dimensions the value of $b = 0.75$ holds, while growing in 2 or 1 dimension(s) decreases the value of b. Interestingly, scaling considerations based on surface-area relationships, such as DEB, predict the opposite pattern; a lower dimensionality of ontogenetic growth due to increased elongation or shape flattening will increase the value of b (Kearney and White 2012). Hirst et al. (2014) show that the relationship between the dimensionality of ontogenetic growth and the scaling exponent for metabolic rate, b, matches with predictions based on surface-area theory and refutes the prediction of resource-transport network models (see also Glazier et al. 2015). So DEB and MTE can both harbor variation in the ontogenetic scaling of metabolism with body size, but DEB seems to do a better job in explaining the existing patterns of variation (Glazier et al. 2015; Hirst et al. 2014, 2017).

Although there is substantial variation in b and current theories of metabolic organization predict variation in b due to changes in the dimensionality of ontogenetic growth, there is currently no understanding about the adaptive significance of this variation (but see Ohlberger et al. 2012*b* and Glazier et al. 2015 for empirical examples). Variation in the scaling of metabolic rate over ontogeny ultimately stems from variation in the scaling of the processes that contribute to metabolic rate. These are processes related to energy supply (assimilation which fuels growth) and energy expenditure (maintenance metabolism). Okie (2013) shows that such variation can occur through adaptations that change the surface-area to volume scaling ratio, such as fractal-like surface convolutions, shape shifting through elongation, flattening and hollowing or internalization of surfaces. When applied to digestive surface areas, such adaptations can alter the scaling of assimilation rate with body mass (Okie 2013). Understanding the selection pressures on the scaling of assimilation and maintenance metabolism will contribute to understanding observed variation in b.

Here, we use a dynamic energy budget model to study the adaptive consequences of changes in the ontogenetic body size scaling of two processes that contribute signif-

icantly to metabolic rate: energy supply (assimilation) and maintenance metabolism. Assimilation depends on food density through a type-II functional response, which depends on two processes that each have a separate scaling relation with body size: the maximum ingestion (*i.e.* digestion) rate and the attack rate. Together with the scaling of maintenance metabolism there are in total three different scaling exponents: maximum ingestion scaling, attack rate scaling and maintenance rate scaling. We study selection on each of these exponents in dependence on the other two exponents. To constrain the possible evolutionary outcomes, we use either one of the two different trade-offs: a juvenile-adult trade-off or an energetic trade-off. Under a juvenile-adult trade-off an increase in a scaling exponent leads to an increase of the relevant process for adults, but to a decrease for juveniles. With the energetic trade-off, changing a scaling exponent leads to a response of the relevant process in the same direction for all differently sized organisms. There are, however, energetic costs associated with the maximum ingestion rate and attack rate. These costs represent metabolic costs of maintaining a large digestive machinery (for a higher maximum ingestion) and activity costs (for a higher attack rate).

Our approach builds on a recent analysis by Hin and De Roos (in prep.), who studied the adaptive dynamics of the ontogenetic scaling of maximum ingestion and maintenance metabolism, but implicitly assumed that the attack rate has an identical scaling as the maximum ingestion rate and only used a juvenile-adult trade-off. With these assumptions, Hin and De Roos (in prep.) found strong selection towards an equal scaling of maximum ingestion rate and somatic maintenance requirements with body size. Furthermore, the common exponent of both processes depended on the extent of pre- versus post-maturation growth and on the size-dependency of the mortality rates (Hin and De Roos in prep.). The model we present here is a more general size-structured consumer-resource model that under specified conditions simplifies to the model as studied by Hin and De Roos (in prep.). We show that the identical scaling of attack and maximum ingestion rates as assumed by Hin and De Roos (in prep.) is actually an evolutionary outcome of our more general model. In addition, this outcome is independent of the assumed trade-off. In contrast, the choice of trade-off does influence the evolved outcome of the scaling of energy supply (both maximum ingestion and attack rate) in relation to energy expenditure and we discuss the reason for this. Furthermore, we discuss how these results relate to the variation in the scaling of metabolic rate with body size.

3.2 – Model and method

Model description

We build upon and extend the model as presented by Hin and De Roos (in prep.) who study the evolution of the scaling of maximum ingestion and maintenance metabolism with body size under a juvenile-adult trade-off. We refer the reader to Hin and De Roos (in prep.) for a detailed motivation and description of the modeling approach. All model equations are summarized in table 3.1 and here we will only shortly summarize the model components and highlight the important extensions compared to the model by Hin and De Roos (in prep.).

We use the modeling framework of physiologically structured population models (De Roos 1997; De Roos et al. 1992; Metz and Diekmann 1986). In this framework all assumptions pertain to the details of the individual-level energy budget, which describes the rate of resource ingestion, assimilation, growth and reproduction as a function of body mass s and resource density R. Resource ingestion, $I(R, s)$, follows a type-II functional response of resource density with maximum ingestion rate $M\left(\frac{s}{s_r}\right)^Q$. In this power law function Q is the scaling exponent of maximum ingestion with body mass s and M represents the maximum ingestion rate of an individual with size s_r. In the model of Hin and De Roos (in prep.) the half-saturation constant of the functional response describing resource ingestion is assumed to be independent of body size. Since the half-saturation density in the type-II functional response is equal to the ratio of the maximum ingestion rate and the attack rate, this assumption implies that the attack rate scales in an identical way with body mass as the maximum ingestion rate. Our first modification is to relax this identical scaling assumption in the model by Hin and De Roos (in prep.) by introducing a separate power law scaling function for the attack rate with body mass: $A\left(\frac{s}{s_r}\right)^X$. Similar to the maximum ingestion rate, the scaling of the attack rate is determined by the scaling exponent X, while the constant A sets the attack rate of an individual of mass s_r. The half-saturation density hence equals: $\frac{M}{A}\left(\frac{s}{s_r}\right)^{Q-X}$, which leads to the following expression for the ingestion rate as a function of body size:

$$I(R, s) = \frac{M\left(\frac{s}{s_r}\right)^Q R}{R + \frac{M}{A}\left(\frac{s}{s_r}\right)^{Q-X}}$$

By setting $X = Q$ this expression reduces to the formulation used by Hin and De Roos (in prep.).

Resource assimilation rate equals the product of the ingestion rate and the conversion efficiency σ, which accounts for assimilation efficiency and costs of specific-dynamic action (De Roos and Persson 2013). Biomass production rate is denoted by

Table 3.1 – Model Equations

Equation	Description
$I(R, s) = M\left(\frac{s}{s_r}\right)^Q \frac{R}{R + \frac{M}{A}\left(\frac{s}{s_r}\right)^{Q-X}}$	Resource ingestion
$\Omega(R, s) = \sigma I(R, s) - T\left(\frac{s}{s_r}\right)^P - c_A A\left(\frac{s}{s_r}\right)^X - c_M M\left(\frac{s}{s_r}\right)^Q$	Biomass production
$g(R, s) = \begin{cases} \Omega^+(R, s) & \text{for } s < s_j \\ \kappa(s)\Omega^+(R, s) & \text{for } s \geq s_j \end{cases}$	Growth rate
$b(R, s) = \begin{cases} 0 & \text{for } s < s_j \\ \frac{(1-\kappa(s))\Omega^+(R,s)}{s_b} & \text{for } s \geq s_j \end{cases}$	Fecundity rate
$\kappa(s) = \begin{cases} 1 - 3L(s)^2 + 2L(s)^3 & \text{for } s_j \leq s < s_m \\ 0 & \text{for } s = s_m \end{cases}$	Allocation function
with $L(s) = \frac{s-s_j}{s_m-s_j}$	
$\mu(R, s) = \mu_c - \frac{\Omega^-(R, s)}{s}$	Mortality rate
$G(R) = \delta\,(R_{max} - R)$	Resource growth rate

We use $\Omega^+(R, s)$ to denote $\max(\Omega(R, s), 0)$ and $\Omega^-(R, s)$ means $\min(\Omega(R, s), 0)$

$\Omega(R, s)$ and equals the difference between assimilation rate and the energy expenditure on metabolic maintenance costs. The second extension that we introduce to the model of Hin and De Roos (in prep.) is the inclusion of activity costs and fixed costs for maximum ingestion capacity. We assume that increased foraging activity increases the attack rate, which leads to increased ingestion rate at low resource density. However, increased activity does not come for free, but at the expense of higher metabolic costs. We therefore include in the metabolic costs a component that is proportional to the attack rate function with proportionally constant c_A. Similarly, an increased maximum ingestion rate is assumed to require maintaining and carrying around a larger digestive machinery, which increases metabolic costs. This trade-off implies costs that are fixed (not dependent on the amount of ingested food). We thus include a component in the metabolic costs that is proportional to the maximum ingestion rate with a proportionally constant c_M. As in the original model in Hin and De Roos (in prep.) other metabolic maintenance costs are modeled by $T\left(\frac{s}{s_r}\right)^P$. The biomass

production rate then becomes

$$\Omega(R, s) = \sigma I(R, s) - T\left(\frac{s}{s_r}\right)^P - c_A A\left(\frac{s}{s_r}\right)^X - c_M M\left(\frac{s}{s_r}\right)^Q \tag{3.1}$$

For $c_A = 0$ and $c_M = 0$, in addition to $X = Q$ we retrieve the model of Hin and De Roos (in prep.).

Similar to Hin and De Roos (in prep.) the biomass production, when positive, is entirely used for growth by juvenile individuals ($s < s_j$). Adults ($s \geq s_j$), allocate a size-dependent fraction $\kappa(s)$ to growth and use the remaining fraction $1 - \kappa(s)$ for reproduction. The allocation function $\kappa(s)$ is a sigmoid function that decreases from 1 at $s = s_j$ while reaching zero at $s = s_m$ and hence sets the asymptotic body mass that individuals attain when resource density is sufficient (table 3.1). Individuals suffer from size-independent background mortality μ_c and starvation mortality when ingested resource biomass is insufficient to cover metabolic requirements (*i.e.* $\Omega(R, s) < 0$). The magnitude of the starvation mortality is equal to the mass-specific biomass production when negative (table 3.1). Resource growth follows semi-chemostat dynamics with turn-over rate δ and maximum resource density $R_{\max}$ (table 3.1).

Our ecological system boils down to a single size-structured consumer that feeds on an unstructured food resource. This consumer-resource interaction is the single feedback loop in the model. Ecological theory stipulates that in such a consumer-resource setting the consumer phenotype that can suppress the resource density to the lowest level, will win competition (Tilman 1980). Evolutionary dynamics of the consumer's phenotype will hence converge towards the point that has minimum resource density in equilibrium. In the terminology of adaptive dynamics this point is a continuously stable strategy (Eshel 1983), which is a convergence and evolutionarily stable singular strategy (Geritz et al. 1998).

Model Parameterization

All model parameters are summarized in table 3.2 and we refer to Hin and De Roos (in prep.) for a more thorough description of their derivation. To allow for a direct comparison with the model by Hin and De Roos (in prep.) we adopt their parameter values for $R_{\max}$, δ, M, T, μ_c and σ (table 3.2), which are in turn based upon the parameterization described in De Roos and Persson (2013). Consumer body mass is expressed in grams, while resource biomass density is expressed in milligram per liter (see also De Roos and Persson 2013). The default value for the attack rate constant A is derived from the fact that the half-saturation constant equals the ratio between maximum ingestion rate and attack rate. Hin and De Roos (in prep.) use a value of 0.1 and 3 for the maximum ingestion rate and half-saturation constant, respectively. We hence adopt a default value of 0.033 for the attack rate constant A. The use of gram

Table 3.2 – Model Parameters

Symbol	Units	Value	Description
R_{max}	$mg\ L^{-1}$	30	Maximum resource density
δ	day^{-1}	0.01	Resource renewal rate
Q	–	varies	Maximum ingestion exponent
X	–	varies	Attack rate exponent
P	–	varies	Maintenance exponent
M	$g\ day^{-1}$	0.1	Maximum ingestion constant
T	$g\ day^{-1}$	0.01	Maintenance constant
A	$L\ day^{-1}\ g\ mg^{-1}$	0.033	Attack rate constant
μ_c	day^{-1}	0.0015	Background mortality
σ	–	0.5	Assimilation efficiency
c_A	$mg\ L^{-1}$	0	Constant in attack rate trade-off
c_M	–	0	Constant in maximum ingestion trade-off
s_b	g	0.1	Size at birth
s_j	g	1	Size at maturation
s_r	g	1	Scaling reference size
s_m	g	10	Maximum size

as the unit for consumer body mass and milligram in the unit for resource density, gives the attack rate the dimension of L day^{-1} g mg^{-1}.

In case of an energetic trade-off, the proportionality constant c_A and c_M are chosen based on two considerations. The first is that c_M is a dimensionless constant that should not exceed the value of the assimilation efficiency to guarantee a positive biomass production rate under unlimited food supply. The feasible range for c_M is hence $0.0 - 0.5$ and we adopt a default value of 0.1. The second consideration is that field metabolic rates are estimated to be approximately 2.5 times the resting metabolic rate (Peters 1983). Hence, for an individual of size s_r we can write $c_A A + c_M M + T = 2.5\ T$, which for the default values for A, M and T and $c_M = 0.1$, gives $c_A = 0.15$.

Model Analysis

Model analysis was done with PSPManalysis (De Roos 2016), a software package especially designed for equilibrium and evolutionary analysis of physiologically structured population models. A short description of the methodology of PSPManalysis can be found in Hin and De Roos (in prep.) and more detailed information and references are

given at https://bitbucket.org/amderoos/pspmanalysis. The PSPManalysis package is used to solve the canonical equation of adaptive dynamics (Dieckmann and Law 1996; Durinx et al. 2008). This equation gives an approximate rate of trait change under evolutionary selection and is a function of the selection gradient and a factor, which scales the rate of evolution and includes the population birth rate, the occurrence rate of new mutants and, in case of multiple evolving traits, the mutational covariance matrix. In adaptive dynamics, the selection gradient equals the derivative of mutant invasion fitness in the equilibrium as set by the resident, evaluated at the resident trait value (Geritz et al. 1998). Since we are interested in the qualitative outcome of the evolutionary dynamics, we plot evolutionary trait change as a function of scaled time by setting time equal to 1 when the selection gradient becomes smaller than 10^{-8}. This makes the unit of evolutionary time dependent on the magnitude of the selection gradient, but never changes the qualitative outcome of evolutionary dynamics. We furthermore assume an identical mutation probability for all evolving traits and in case of multiple evolving traits, the mutational covariance matrix is assumed equal to the identity matrix. The PSPManalysis package is also used to continue the population dynamical equilibrium as a function of a model parameter. It furthermore detects evolutionarily singular strategies (ESS) along such an equilibrium curve and classifies these ESSs according to the classification of Geritz et al. (1998). We assessed the non-equilibrium dynamics, such as population cycles, by using numerical integration of the cohort dynamics with the Escalator Boxcar Train method (De Roos 1988; De Roos et al. 1992).

We first study the case of a juvenile-adult trade-off by adopting the size at maturation for the scaling reference size ($s_r = s_j$) and specifying no metabolic costs for activity and maximum ingestion ($c_A = c_M = 0$). Under a juvenile-adult trade-off an increase in the exponents Q, X or P will lead to an increase in maximum ingestion, attack rate and maintenance metabolism, respectively, for adults ($s \geq s_j$) and a concomitant decrease for juveniles ($s < s_j$). In this setting, we study whether the separate scaling for the attack rate influences the results of Hin and De Roos (in prep.). We subsequently adopt an energetic trade-off instead of a juvenile-adult trade-off by setting $s_r = s_m$. With this choice of s_r, changing the scaling exponents Q, X and P will both affect the size-dependency and the overall level of the maximum ingestion rate, the attack rate and maintenance rate, respectively. The overall rates of these processes are also determined by the scaling constants, M, A and T. Selection on the scaling exponents Q, X and P will therefore depend on the values of the scaling constants M, A and T, respectively. To prevent confounding effects of the scaling constants on the evolution of the scaling exponents, we allow the scaling constants to evolve in concert with the associated scaling exponent in case of the maximum ingestion rate and the attack rate. This implies that we explore two-dimensional evolutionary sin-

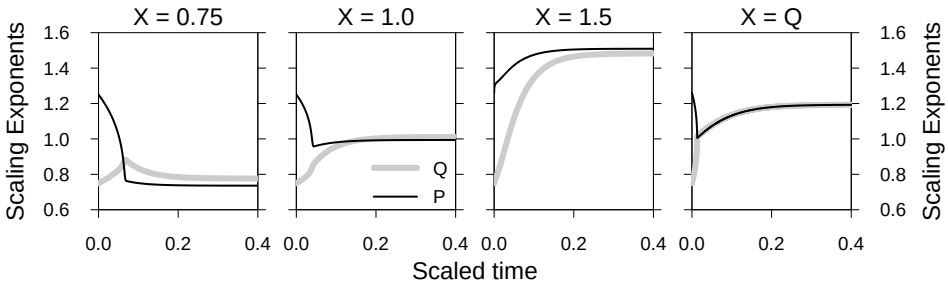

Figure 3.1 – Evolutionary change in scaling exponents of maximum ingestion (Q; gray line) and maintenance (P; black line) as a function of scaled evolutionary time for different values of the attack rate exponent (X; indicated above each panel). In the right-most panel the maximum ingestion and attack rate exponents are equal and the gray line corresponds to both Q and X. Default parameters as shown in table 3.2 are used. The juvenile-adult trade-off is assumed ($s_r = s_j = 1$) and there are no costs of activity or maximum ingestion ($c_A = c_M = 0$).

gular strategies (an evolutionary equilibrium for two traits) containing both a scaling constant (M or A) and a scaling exponent (respectively Q and X). Subsequently we study the dependence of such two-dimensional CSSs on the other scaling exponents.

3.3 – Results

Juvenile-adult trade-off

Hin and De Roos (in prep.) found that under a juvenile-adult trade-off ($s_r = s_j$ and $c_A = c_M = 0$) selection on the scaling exponents of maximum ingestion and maintenance metabolism with body size leads to identical values of these two scaling exponents. We explore here how this result depends on the assumption by Hin and De Roos (in prep.) that the half-saturation constant is independent of body size. This is identical to assuming that the attack rate and maximum ingestion rate scale in an identical fashion with body size ($Q = X$). In figure 3.1 we show the evolutionary dynamics of the maximum ingestion exponent (Q) and the maintenance exponent (P) as a function of scaled time for different values of the attack rate exponent (X). Starting from different initial values, the maximum ingestion and maintenance exponents reach an evolutionary equilibrium (CSS) that depends on the value of the attack rate exponent. Overall, increasing values of the attack rate exponent (X) select for higher values of the maximum ingestion and maintenance exponents (Q and P). For $X = 0.75$ and $X = 1$, the CSS-value of the maximum ingestion exponent (Q) exceeds the CSS-value for the maintenance exponent (P) and vice versa for $X = 1.5$. However, the difference between the CSS-values of the maximum ingestion and maintenance exponents is small compared to the extent both exponents change with changing values

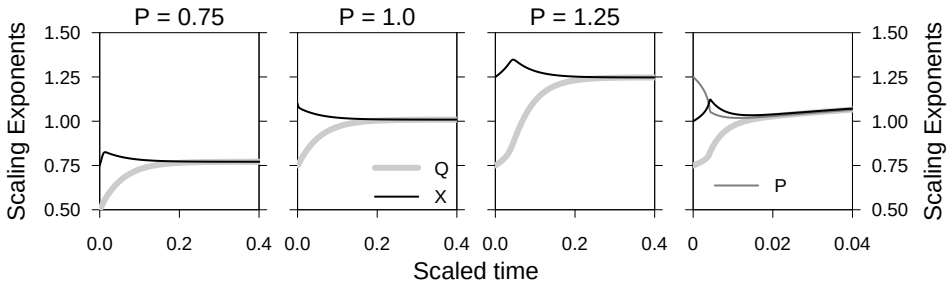

Figure 3.2 – Evolutionary change in the scaling exponents of maximum ingestion (Q; gray line) and attack rate (X; black line) as a function scaled of evolutionary time for different values of the maintenance rate exponent (P; indicated above each panel). Selection leads to convergence of Q and X, irrespective of P. An increased maintenance scaling does increase the evolved scaling exponents of maximum ingestion (Q) and attack rate (X). In the right-most panel all three exponents evolve simultaneously and reach a stable evolutionary equilibrium (CSS). Note that in this panel the x-axis scaling is different from the other panels to better show the transient dynamics. All other parameters as in figure 3.1.

for the attack rate exponent (X). For comparison we also show the case where $X = Q$ (figure 3.1; see also Hin and De Roos in prep.). In this case the evolutionary dynamics consist of two parts. The first part is the rapid convergence of both scaling exponents and in the second part, the selection on the maintenance exponent P reverses and both exponents asymptotically approach a CSS. In this CSS, both exponents are equal to ± 1.19 (Hin and De Roos in prep.). Figure 3.3 (left panel) shows the CSS-values of the maximum ingestion and maintenance exponents (Q and P) as a function of the attack rate exponent (X). At the threshold value of $X = 1.19$ the CSS-values of Q and P intersect each other and simultaneously intersect the diagonal. In this point all three exponents are in evolutionary equilibrium (all selection gradients are equal to zero). In accordance with figure 3.1, the CSS-value of Q exceeds the CSS-value of P for low X-values ($X < 1.19$) and vice versa for large X-values ($X > 1.19$; figure 3.3).

Figure 3.2 shows evolutionary change over scaled time of both the maximum ingestion (Q) and attack rate exponent (X) for different values of the maintenance exponent (P). Independent of the maintenance scaling, the maximum ingestion and attack rate exponents convergence to a CSS-point in which they are equal. The common value of both exponents in this CSS closely follows the maintenance scaling (P), but are only exactly equal to the maintenance exponent at $P \approx 1.19$ (figure 3.3; right panel). At this point, all three scaling exponents are in evolutionary equilibrium (similar to figure 3.3; left panel). For $P < 1.19$ the CSS-values of Q and X are larger than P (above the diagonal), while for $P > 1.19$ they are smaller than P (below the diagonal). Therefore, deviating from the assumption by Hin and De Roos (in prep.)

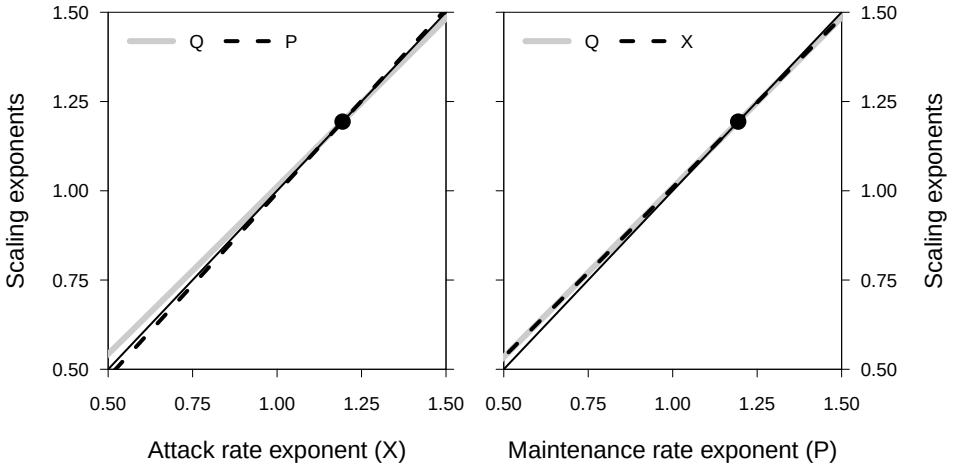

Figure 3.3 – The evolutionary equilibrium (CSS) of Q and P as function of X (left panel), and the evolutionary equilibrium (CSS) of Q and X as a function of P (right panel). The thin black line indicates the diagonal and the black dot is where the diagonal is crossed by the evolutionary equilibrium. At this point selection on the x-axis variable vanishes and all three exponents are at evolutionary equilibrium. A juvenile-adult trade-off is assumed ($s_r = s_j = 1$), and all other parameters are as denoted in table 3.2.

of an identical scaling of attack rate and maximum ingestion rate with body size, changes the evolutionary dynamics of Q and P, but this effect is only small. On the other hand, it appears that $Q = X$ is itself an evolutionary outcome, irrespective of the value of P. The assumption by Hin and De Roos (in prep.) that the scaling exponent of the maximum ingestion rate (Q) and the attack rate (X) are the same, boils down to assuming that they are both in evolutionary equilibrium. As a consequence, when all three exponents evolve (right-most panel in figure 3.2), all the results derived by Hin and De Roos (in prep.) apply. That study furthermore shows how the evolved scaling value of 1.19 changes with patterns of pre- and post-maturation growth and size-specific mortality rates.

Energetic trade-off

As an alternative to the juvenile-adult trade-off that underlies the results by Hin and De Roos (in prep.), we explore a trade-off between energy supply and energy expenditure. Setting c_A and c_M to positive values imposes metabolic costs for increased activity and maximum ingestion capacity. To avoid that the two different trade-offs operate simultaneously, we adopt $s_r = s_m$. Since the reference body size is now an order of magnitude larger ($s_m/s_j = 10$), default values for the scaling constants M, A, and T, which reflect the maximum ingestion, attack and maintenance rate of an individual

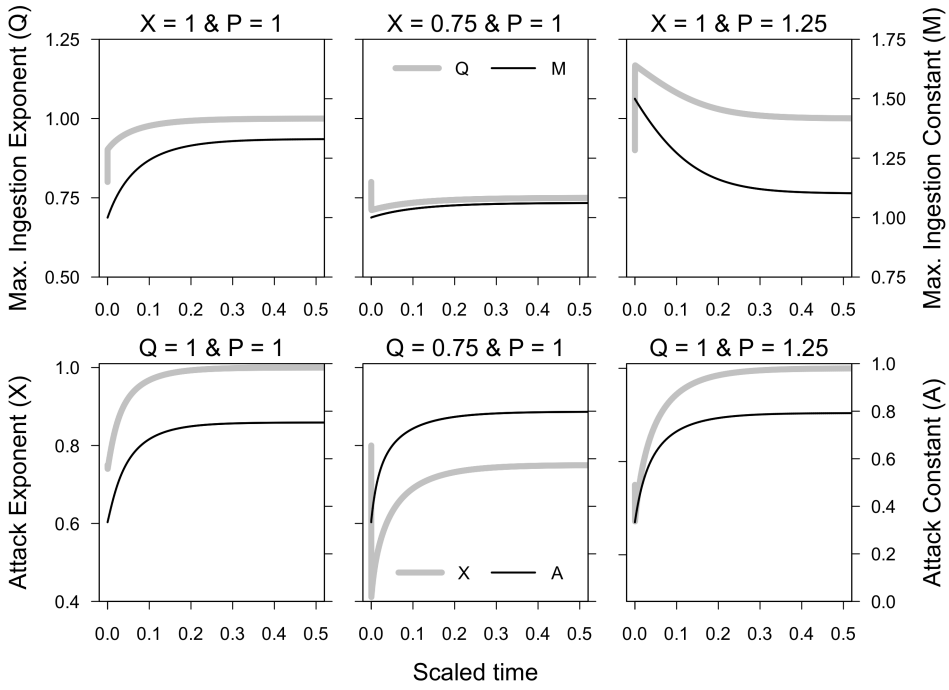

Figure 3.4 – Evolutionary dynamics of the maximum ingestion exponent and constant (Q and M; top panels) and the attack rate exponent and constant (X and A; bottom panels) in case of an energetic trade-off, for different values of the other two exponents (respectively X or Q, and P as indicated above each panel). The scaling exponents related to energy supply (maximum ingestion rate Q or attack rate X) always evolve towards the same value (*i.e.* the fixed value of the other supply related exponent, attack rate X and maximum ingestion rate Q, respectively). This is independent of the value of the maintenance rate exponent (P). The scaling exponents (Q and X) are shown on the left y-axis, while the scaling constants (M and A) are shown on the right y-axis. All parameters as in table 3.2 in addition to $s_r = s_m = 10$, $c_A = 0.15$, $c_M = 0.1$, $M = 1$, $T = 0.1$ and $A = 0.33$.

with reference body size s_r, will be taken 10 times larger as well. This ensures that the change in reference body size from s_j to s_m does not affect the maximum ingestion rate, attack rate and maintenance metabolic rate when the scaling exponents of these processes are one. By adopting $s_r = s_m$, an increase in the scaling exponent Q, X or P will lead to a decrease in the maximum ingestion rate, attack rate and maintenance rate for all individuals in the consumer population. This effect is not equally strong for all differently sized individuals, but increases with the difference between the maximum and the current body size, $s_m - s$, and is zero at $s = s_m$. A trade-off between energy supply and expenditure arises because food intake is determined by the attack rate and the maximum ingestion rate but in addition depends on the resource density

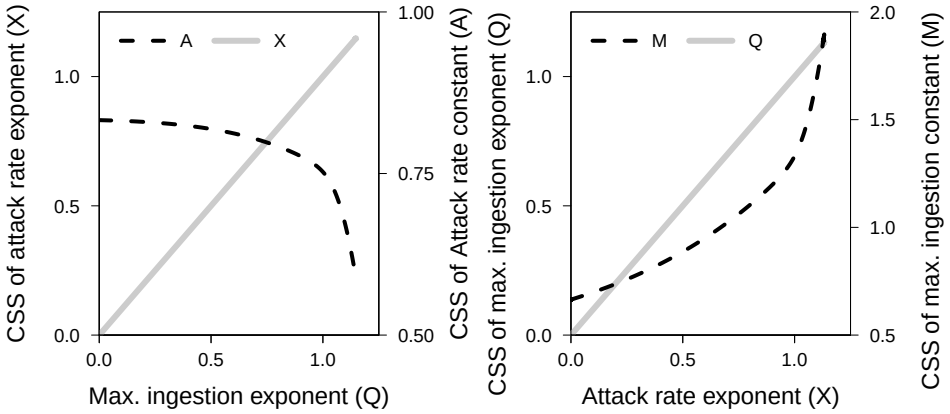

Figure 3.5 – Left panel: evolutionary stable equilibrium values (CSS) of the attack rate scaling exponent (X) and constant (A), as function of the scaling exponent of maximum ingestion rate Q. Right panel: CSS-values of maximum ingestion scaling exponent (Q) and constant (M), as a function of the scaling exponent of attack rate X. In both panels, the evolving scaling exponents (gray lines) are exactly equal to the non-evolving exponent on the x-axis. The scaling exponents (Q and X) are shown on the left y-axis, while the scaling constants (M and A, black dashed lines) are shown on the right y-axis. All parameters as in figure 3.4.

following a type-II functional response. The costs of increased attack rate and/or maximum ingestion capacity, however, have to be paid always, irrespective of resource densities. At low resource density the energy supply is limited by the value of the attack rate. For high resource density, the asymptotic level of the functional response, which is set by the maximum ingestion rate, is the main limiting factor. Increasing the attack rate will increase the limitation by maximum ingestion, and vice versa, increasing the maximum ingestion will lead to a stronger limitation by the attack rate. Increasing both attack rate and maximum ingestion rate will lead to ever increasing rates of energy supply and we will hence refrain from evolving these two parameters simultaneously.

Changing the scaling exponents of attack rate (X) and maximum ingestion (Q) will not only change the size-dependency of the functional response parameters, but also their overall value across the whole size distribution. Selection on the scaling exponents of attack rate (X) and maximum ingestion (Q) is thus confounded by the value of the scaling constants A and M. To avoid such confounding effects we always let the scaling exponents evolve together with their corresponding scaling constants (figure 3.4). Over evolutionary time the value of the evolving scaling exponent related to energy-supply (maximum ingestion Q or attack rate X) always approaches the value of the non-evolving exponent related to energy supply, attack rate X or maximum in-

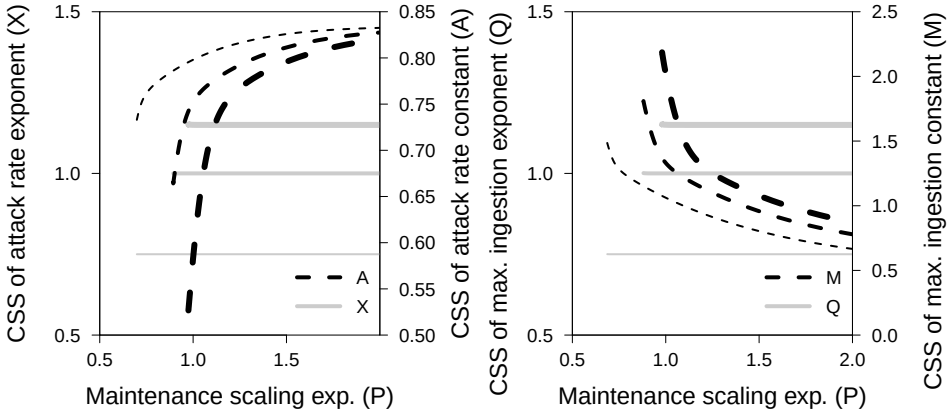

Figure 3.6 – Left panel: evolutionary stable equilibrium values (CSS) of the scaling exponent and constant of attack rate, X and A, respectively, as a function of the scaling exponent of maintenance rate P, for different values of the scaling exponent of maximum ingestion rate: $Q = 0.75$ (thin lines), $Q = 1$ (normal lines) and $Q = 1.15$ (thick lines). Right panel: evolutionary stable equilibrium values (CSS) of the scaling exponent and constant of maximum ingestion rate, Q and M, as a function of the scaling exponent of maintenance rate P, for different values of the scaling exponent of attack rate: $X = 0.75$ (thin lines), $X = 1$ (normal lines) and $X = 1.15$ (thick lines). The evolving exponents (gray lines), are not influenced by the value of the maintenance exponent (P; x-axis). The population goes extinct when the maintenance rate becomes too high (low values of P). Scaling exponents Q and X are shown on the left y-axis, while scaling constants (M and A, black dashed lines) are shown on the right y-axis. All other parameters as in figure 3.4.

gestion Q, respectively. This is independent of the maintenance rate exponent (P; figure 3.4). This result is corroborated by figure 3.5 and figure 3.6, that show the evolutionary equilibrium value of each parameter pair, consisting of the scaling exponent and the constant of the attack rate or the maximum ingestion rate, as a function of either the other, non-evolving energy-supply exponent (maximum ingestion rate exponent Q or attack rate exponent X, respectively; figure 3.5) or of the maintenance rate exponent P (figure 3.6). Indeed, figure 3.5 (left panel) confirms that the evolutionary stable value of the scaling exponent of the attack rate exactly equals the scaling exponent of the maximum ingestion rate, when the latter does not evolve. Vice versa, the evolutionary stable value of the scaling exponent of the maximum ingestion rate is exactly equal to the (non-evolving) attack rate exponent (figure 3.5; right panel). Hence, similar to the result obtained with a juvenile-adult trade-off also in case of a trade-off between energy supply and expenditure we find as evolutionary outcome that $Q = X$. Furthermore, this result is independent of the value of the maintenance rate exponent (P), as changing P has no effect on the evolutionary stable values of

the scaling exponents of attack rate X or the maximum ingestion rate Q (figure 3.6). This result differs from the case of the juvenile-adult trade-off, where the maintenance rate scaling had a strong effect on the evolved body size scaling of maximum ingestion and attack rate (figure 3.3; right panel). However, under a juvenile-adult trade-off both the maximum ingestion and attack rate scaling could evolve, while under an energetic trade-off the evolution of these scaling exponents leads to ever increasing rate of energy supply.

3.4 – Discussion

The model presented here shows that selection on the scaling of metabolic processes with body mass leads to convergence of the scaling exponents of the processes related to energy-supply, independent of the type of trade-off that is considered. These are the maximum ingestion rate, which determines the rate of food ingestion at unlimited food supply, and the attack rate, which describes the rate at which ingestion increases with food density when food density is low. Furthermore, under a juvenile-adult trade-off the scaling of energy supply and energy expenditure (as represented by maintenance metabolism) converge towards the same body mass scaling over evolutionary time. Under an energetic trade-off, however, the evolutionary stable scaling exponents related to energy supply (either maximum ingestion or attack rate scaling) are independent of the scaling exponent of energy expenditure (maintenance metabolism).

The evolutionary outcome of identical maximum ingestion and attack rate scaling exponents, implies that the half-saturation constant of the functional response, which equals the ratio between maximum ingestion and attack rate, is independent of body mass. Consequently, the functional responses of differently sized individuals have the same qualitative shape and only differ from each other by a factor that depends on body size, but not on resource density. The effect of body mass on half-saturation density has been studied on an interspecific level by both Hansen et al. (1997) and Rall et al. (2012), who both concluded that in freshwater and marine invertebrates the half-saturation density is constant with species body mass. However, for species from other ecosystems and metabolic types there is no consistent picture, as half-saturation densities can either increase of decrease with species body mass (Rall et al. 2012). The analysis of Rall et al. (2012) furthermore showed that attack rates and handling times (the inverse of maximum ingestion) show signs of a humped-shaped relationship with body mass. This pattern also arises in the attack rates of several species of fish, when comparing differently sized individuals of the same species (Byström et al. 2004; Hjelm and Persson 2001; Jansen et al. 2003). Attack rates are known to depend on a number of factors, such as prey body size, structural complexity of the habitat, swimming speed and visual accuracy (Rall et al. 2012). These multitude of external and internal

influences can lead to a more complex relationship between attack rate and body size than the power law relation assumed in this study. Further research should point out how external factors shape selection on attack rates and therefore affect the scaling of the half-saturation constant with body size. In our model, fitness relates to the ability of the consumer to suppress and persist on the lowest resource density and we therefore conclude that population-level resource use is an important factor to consider when studying the evolution of attack rates and handling times.

With respect to the scaling exponents of energy supply (attack rate and/or maximum ingestion rate) and energy expenditure, the evolutionary outcomes differ between the different trade-offs investigated. As already found by Hin and De Roos (in prep.), these processes converge towards the same scaling with body size in case of a juvenile-adult trade-off. As a result, the maintenance resource density (MRD), which is the amount of resources required to cover maintenance metabolism, becomes independent of body mass. This precludes the occurrence of starvation and neutralizes size-dependent intraspecific competition (Hin and De Roos in prep.). However, the size-independence of the MRD does not imply that differently sized individuals are equally efficient in converting ingested resource into new biomass. First, larger individuals will have higher foraging rates and hence also higher production rates of new biomass. Second, as the scaling exponents of the energy supply and energy expenditure do not necessarily converge to one (see figure 3.1; right panel), also the mass-specific biomass production rate (MBP) changes with body size. As shown by Hin and De Roos (in prep.), the value of the common scaling exponent is dependent on the size-specific mortality and the extent of pre- and post-maturation growth. The results in this paper show that the outcomes presented by Hin and De Roos (in prep.) are robust against the incorporation of a separate attack rate scaling.

That the scaling exponents of energy supply (either maximum ingestion or attack rate) and energy expenditure evolve to different values in case of an energetic trade-off (figure 3.6) relates to the fact that selection is only stabilizing when a single scaling exponent related to energy supply evolves. Simultaneous evolution in both attack rate and maximum ingestion rate would always lead to a run-away evolutionary process with ever increasing value of the functional response, which is clearly unrealistic. Evolutionary change in one exponent (and associated constant) is thus only stabilizing when the other exponent does not evolve. In addition, with the choice of $s_r = s_m$, an increase in the scaling of maintenance metabolism (P) always leads to a decrease in the maintenance rate for every individual. Hence, selection always favors higher values of P. The energetic trade-off thus provides us with the insight that the scaling exponents of maximum ingestion and attack rate converge over evolutionary time to the same value, irrespective of the choice of the trade-off. Furthermore, it shows that differences in the scaling of energy supply and energy expenditure can only be

understood from the perspective of limited evolvability of two out of the three scaling exponents studied here.

Focusing on the juvenile-adult trade-off we observe that selection on metabolic scaling favors all three scaling exponents to be identical (figure 3.2 and 3.3). Consequently, evolution also favors the scaling of energy supply and energy expenditure to be equal (Hin and De Roos in prep.). This outcome is not in accordance with the MTE, which assumes a value of 0.75 for the scaling exponent of energy supply and an exponent of 1 for energy expenditure. The latter assumption is derived from the logic that each cell (in MTE) requires a fixed maintenance costs (West et al. 2001), which is probably the most parsimonious assumption. Even if the maintenance scaling is fixed, our evolutionary analysis shows that the juvenile-adult trade-off would force the scaling exponents of energy supply (maximum ingestion (Q) and attack rate (X)) to evolve to closely match the linear scaling of maintenance. In DEB theory an increase in energy supply can be achieved by an increase in the surface-area to volume ratio. Many organisms from a wide variety of taxa have indeed evolved adaptations to escape surface-area constraints that occur when growing bigger (Gould 1966; Hirst et al. 2014; Lewis 1976; Okie 2013). The nature and some examples of these adaptations are discussed in Okie (2013), while Hin and De Roos (in prep.) discuss the interpretation of these adaptations in relation to the theoretical result about the convergence of the scaling exponents of energy supply and expenditure over evolutionary time.

How can our approach be related to observed variation in the scaling of metabolic rate with body mass? First of all, it needs to be stressed that the measured scaling of metabolic rate does not directly correspond to any parameter, or combination of parameters in our model. For example, we do not explicitly account for growth overhead costs, which is one of the processes that contributes to the experimentally measured rates of respiration, which are commonly adopted as a measure for metabolic rate (Kooijman 2010). Incorporating such costs of growth in our model would merely rescale the size-at-age curve and does not lead to any qualitative differences in the model outcome. When a fixed proportion of the biomass flow allocated towards growth is spent on the overheads of growth, the energy dissipation rate in our model becomes a linear combination of the growth rate (which scales as the biomass production for juveniles (equation (3.1)) and the maintenance rate. Under a juvenile-adult trade-off, the maximum ingestion and attack rate scaling exponents (Q and X, respectively) become identical to the scaling exponent of the maintenance rate (P) in the evolutionary equilibrium, which would imply that the scaling of the energy dissipation rate for juveniles is equal to the value of this common exponent. As reported by Hin and De Roos (in prep.), this common scaling exponent decreases with increasing juvenile mortality and increasing pre-maturation growth, and decreases with increasing adult mortality and increasing post-maturation growth. In case of the energetic trade-off,

the evolutionary stable scaling exponent of one of the energy supply exponents depends on the value of the other, non-evolving energy supply exponent. Increasing mortality rates of either juveniles or adults do not influence the scaling exponents of energy supply with body size, but only changes the evolution of the constants in these size scalings (results not shown). Changes in the scaling constants might, however, also affect observed variation in metabolic rate when those changes lead to higher growth rates. Because growth rates decrease when body mass increases, an increasing contribution to growth might lead to a decrease in the scaling of metabolic rate. How exactly the scaling constants change the slope of metabolic rate with body mass, and under which conditions, remains a topic for further study. Another source of variation in the metabolic rate under an energetic trade-off stems from the variation in the constrained (non-evolving) scaling exponents that drive evolution in the other scaling exponents. Thus, observed variation in the measured scaling of metabolic rate with body mass will be more straightforward to relate to our results with a juvenile-adult trade-off than when an energetic trade-off constrains the evolutionary process.

Studies on the adaptive consequences of changes in the scaling exponents of energy supply and energy expenditure with body size are rare (but see Hin and De Roos in prep.). Even though the ecological and evolutionary (fitness) consequences of changes in these scaling exponents can be large because of their effect on population and community dynamics. These higher-level consequences can be understood through the concept of ontogenetic asymmetry in energetics (De Roos et al. 2013). This phenomenon occurs when the mass-specific biomass production (MPB) rate is a non-constant function of body size. In other words, individuals that differ in size also have different mass-specific rates at which they produce new biomass. A size-dependent MPB even occurs when all three scaling exponent are equal, but different from one. When one of the three exponents differs from the other two, also the maintenance resource density (MRD) changes with body mass.

Ontogenetic asymmetry in terms of a size-dependent MRD leads to population cycles, with either juvenile- or adult-driven cycles, depending on whether the MRD increases or decreases with body mass (De Roos and Persson 2003; Persson and De Roos 2013; Persson et al. 1998). For example, when the exponent of energy supply is lower than the exponent of energy expenditure (as in descriptions of ontogenetic growth based on DEB or MTE), the MRD increases with body mass. Small individuals can hence persist at lower resource densities than larger individuals. When all individuals compete for a shared resource this type of asymmetry leads to juvenile-driven population cycles (De Roos et al. 2013). Also, ontogenetic asymmetry underlies the phenomenon of biomass overcompensation, which refers to an increase in (stage-specific) biomass density with increasing mortality rates (De Roos et al. 2007). In turn biomass overcompensation is responsible for community-wide effects such as the

emergent Allee effect, facilitation between size-selective predators and alternative stable states (De Roos et al. 2003*b*, 2008*a*; Guill 2009; Van Kooten et al. 2005) . Understanding what drives ontogenetic asymmetry is hence required for understanding their consequences on a population and community level. The present work extends on earlier research by Hin and De Roos (in prep.) that attempts to explain observed patterns of ontogenetic change in energetics from an adaptive point of view. We show that these earlier results are to some extent robust against the introduction into the model of more biological detail, but that model outcomes may differ if a different trade-off is assumed. We conclude that for this approach to be successful, we require a better understanding of the extent to which adaptive evolution can modify the metabolic organization of organisms, and to which extent this process is limited by physiological, physical and developmental constraints.

Acknowledgments

This research was supported by funding from the European Research Council under the European Union's Seventh Framework Programme (FP/2007-2013) / ERC Grant Agreement No. 322814.